Cycloid vs. Harmonic Drives for use in High Ratio, Single Stage Robotic Transmissions

Jonathon W. Sensinger, *Member, IEEE* and James H. Lipsey

Abstract—**Harmonic and cycloid drives are both compact, high ratio transmissions appropriate for use in anthropomorphic robots, although cycloid drives are rarely used in the field. This paper describes the design parameters for cycloid drives and shows the results of six cycloid models designed to match corresponding harmonic drives. Cycloid drive models were compared with manufacturing data from corresponding harmonic drives with respect to maximum gear ratio, transmission thickness, efficiency, backlash/gear ratio ripple, and reflected inertia. Cycloid drive designs were found to be thinner, more efficient, and to have lower reflected inertia than corresponding harmonic drives. However, the cycloid designs had larger gear ratio ripple and substantial backlash, and they could not meet the maximum gear ratio provided by the corresponding harmonic drives in two out of six models for equal applied torques. Two cycloid drives were manufactured to confirm efficiency predictions and demonstrated moderate to high efficiency across a range of output torques. Cycloid drives should be considered for robotic and prosthetic applications where smaller thickness/higher efficiency requirements dominate over low backlash/gear ratio ripple considerations.**

Index Terms—**Cycloid Drive, Harmonic Drive, prosthesis transmission**

I. INTRODUCTION

ROBOTIC electromagnetic actuators are typically coupled to a large reduction transmission to improve the power density of the actuator at the output torque/speed specifications of the robot [1]. Although there are many viable high-reduction gear transmissions, such as stacked planetary gears and cabling systems used in the WAM [2] and PHANTOM [3], the potential for high efficiency, low backlash, and compact form have led many designers to use a single stage high-reduction gear ratio. Many of these designs have used harmonic drives, including the DRL series of robots [4], the Waseda mechanical impedance arm [5], the Liberating Technology Digital Arm, and the authors' previous robots [6, 7]. Harmonic drives achieve a high reduction ratio in a single stage by mating a rigid, slightly elliptical input into a flexible spline (flex-spine) with teeth, coupled to an outer rigid ground that contains two more teeth than the flex-spline [8, 9]. A similar device, termed a cycloid drive [10-12], has been used in power transmissions in boats, cranes, and pumps, but has not been explored for

use in robotics except for in a proprietary prosthetic hand.

Both harmonic and cycloid drives have inputs and outputs that move in opposite directions, and that are coupled by a ball-bearing component between them and an intermediate grounded component that contains more teeth (or lobes) than the output. The two types of devices accomplish similar objectives through different methods (Fig. 1):

- **Cam vs. Ellipse:** The cycloid drive uses an offset cam input, in contrast to the elliptical harmonic drive input, and requires an additional component (output disk) that retains only the rotational movement.
- **Rollers vs. Teeth:** The intermediate component of a cycloid drive uses rollers, in contrast to the teeth of a harmonic drive.
- **Rolling vs. Flexion Strength:** The output of a cycloid drive uses lobes that travel on rollers, creating only compressive stress at the lobe/roller interface. The absence of shear stress at this interface allows the cycloid disk to withstand higher forces. In contrast, the output of a harmonic drive flexes, allowing multiple teeth to mesh simultaneously, in turn increasing the allowable stress the mechanism can withstand.
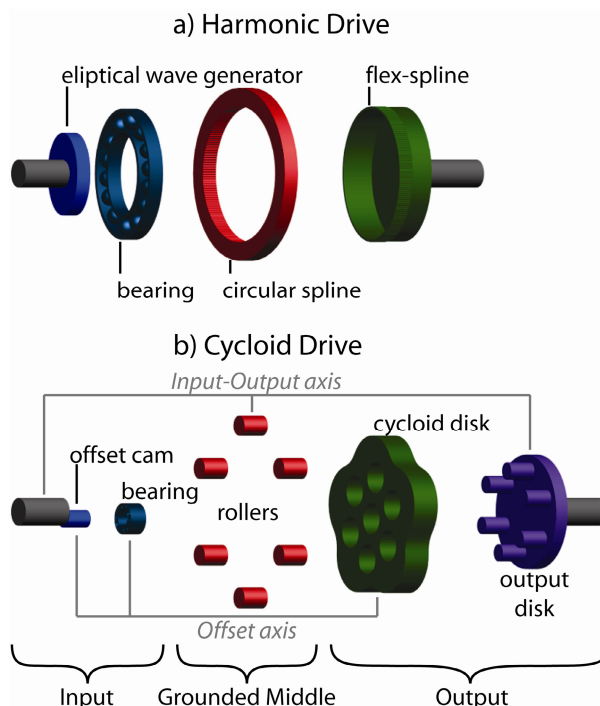

Fig. 1. Harmonic and cycloid drives have many similarities in their operational principles.

Jon Sensinger and James Lipsey are with the Center for Bionic Medicine, Rehabilitation Institute of Chicago, Chicago, IL 60611 (e-mails: sensinger@ieee.org, ieee@lipsey.org).

Harmonic and cycloid drives have both striking similarities and differences, and although trade journals have occasionally offered comments on the superiority of one type vs. the other [13], the majority of these articles contain misconceptions and, for example, do not compare designs with similar gear ratios or applied torque constraints. This article builds on the work of the authors to provide a unified derivation of the relevant attributes of cycloid drives [10]. Using these equations, performance characteristics of cycloid drives may be directly compared with harmonic drives to determine the benefits and weaknesses of each drive type.

II. THEORY

A. Cycloid Parameters & Profile

The single-stage cycloid disk in a cycloid drive has Z_1 lobes (Fig. 2). For the epitrochoid designs considered in this paper, there are Z_2 rollers, where Z_2 is an integer higher than Z_1. The output/input torque gear ratio is:

$$GR = \frac{Z_1}{Z_2 - Z_1} : 1 \tag{1}$$

The rollers have radius R_r, are located at position R away from the center, and the cycloid disk spins about this center on an eccentric cam with radius e. The profile of the cycloid disk is defined by the following equations [11]:

$$C_x = R\cos\phi - R_r\cos(\phi+\psi) - e\cos((Z_1+1)\phi)$$
$$C_y = -R\sin\phi + R_r\sin(\phi+\psi) + e\sin((Z_1+1)\phi) \tag{2}$$

where ϕ is the input angle and ψ is the contact angle between the cycloid lobe and roller, calculated as:

$$\psi = \tan^{-1}\left[\frac{\sin(Z_1\phi)}{\cos(Z_1\phi) - \dfrac{R}{e(Z_1+1)}}\right] \tag{3}$$

A. Cycloid Limitations

Two factors constrain the design of cycloids: the radial forces caused by the eccentric cam, and the feasibility of the geometric profile. These two factors affect the maximum possible gear ratio and the maximum rated torque.
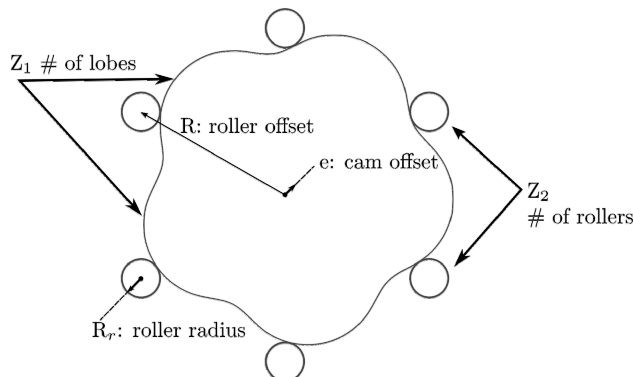

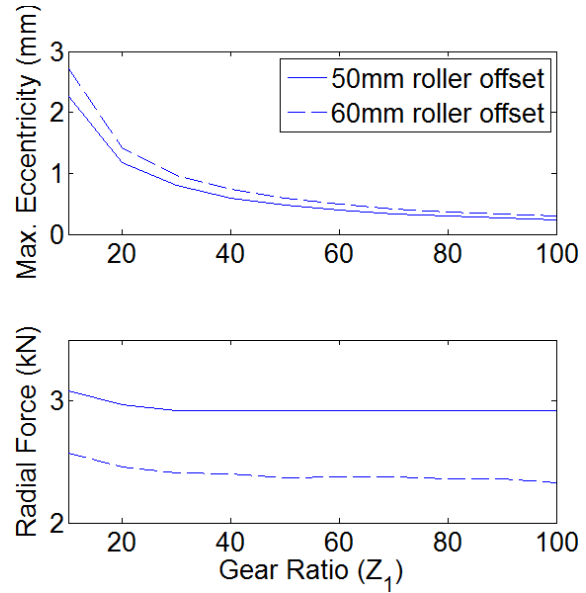Fig. 2. Parameters used to generate cycloid disk profile.

Fig. 3. Radial force is sensitive to roller offset, but insensitive to gear ratio.

Although cycloids generate several large internal forces [10], in the application of these drives to compact, large reduction transmissions, the large radial force caused by the cam eccentricity dominates failure of the device [14]. This radial force is equal to:

$$F_{cam} = \frac{T}{eZ_1} \tag{4}$$

where T is the torque encountered by the gear transmission. This force is highly dependent on the roller offset *(R)*, but relatively insensitive to the gear ratio *(Z₁)*. As the gear ratio decreases for a given output torque, the allowable increase in eccentricity that still avoids undercutting grows proportionally to the increase in force seen due to the decreased gear ratio (Fig. 3).

The maximum gear ratio is indirectly constrained by the radial force, which determines the smallest roller diameter that will not shear under load. The diameter of the rollers and the radius of their offset determine how many rollers may be arrayed before they start to intersect each other [11], which in turn defines the gear ratio.

B. Cycloid Efficiency

Cycloid efficiency is dominated by the interaction of the cycloid disk with the rollers [10]. One of four scenarios is possible.

1) The cycloid profile described by Eq. 2 creates rolling contact between the cycloid disk and circular rollers, even if those rollers are fused to the annulus. The theoretical efficiency of cycloids is accordingly dominated by this rolling contact as follows [10]:

$$\eta = 1 - \mu\frac{R_r}{R} \tag{5}$$

2) Due to machining tolerance offsets in generating a cycloid profile [10], sliding motion is likely to occur

between the cycloid disk and the rollers. If the rollers resist radial loads through internal axles (Fig. 4a), the efficiency will be as follows.

$$\eta = 1 - \mu \frac{R_r}{R_a} , \qquad (6)$$

where R_a is the radius of the internal axle. Commercially available cycloid drives often constrain the rollers in needle roller bearings to achieve even higher efficiency than Eq. 6, but such designs cannot be miniaturized to the compact cycloid designs appropriate for anthropomorphic robots.

3) Supporting the rollers on their outer diameter (Fig. 4b) rather than an internal axle allows for a larger number of smaller diameter rollers to be used, which is often important in robotic designs. If the rollers are housed on the outside, $R_r = R_a$ and the efficiency reduces to:

$$\eta = 1 - \mu , \qquad (7)$$

4) The rollers may be fixed, in which case they may be designed directly into the annulus (Fig. 4c), resulting in fewer parts and tighter tolerance stack-ups. In this case, if sliding motion does occur, the efficiency will be as follows:

$$\eta = 1 - \mu \frac{C}{2\pi} \frac{1}{eZ_1} , \qquad (8)$$

where C is the circumference of the cycloid disk. For each of these cases it is important to note that the efficiency of a cycloid drive is largely independent of applied torque, in contrast to most other gear transmissions, which only have optimal efficiency at maximum torque. This observation has been validated by experimental results [14] and will be evaluated later in this paper.

III. SIMULATIONS

A. Cycloid Design Generation to Match Harmonic Drives

Cycloid profiles generated from the design process described in [10] were compared with manufacturer data parameters from two series of harmonic drives with a range of outer diameters and thicknesses suitable for anthropomorphic robots (Table 1). These series included the Harmonic Drive Inc. (Peabody, MA) CSD set, which is thin but has a minimum outer diameter of 50 mm, and their CSF set, which is thicker but can accommodate an outer diameter of 21 mm.
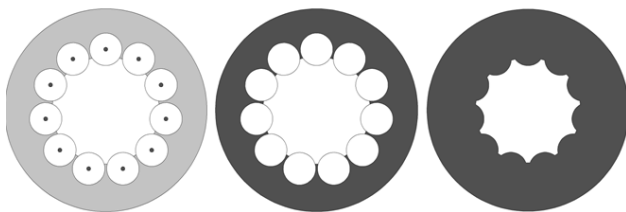
a) Internal-axle   b) External housing   c) Fused rollers

Fig. 4. Roller options. Rollers can be (a) grounded by an internal axle, (b) grounded by the external housing, or (c) fused to the annulus. Dark-gray shading represents the connection between the rollers and the annulus.

Table 1
Harmonic Drive Characteristics

		Outer Diameter	Thickness	Mass	Gear Ratio range	Maximum Momentary Peak Torque
		mm	*mm*	*g*		*Nm*
HD-CSF	5	21	16	35	30 - 100	0.9 - 2.7
	8	31	30	130	30 - 100	3.3 - 9
	11	41	37	240	30 - 100	8.5 - 25
HD-CSD	14	50	11	60	50 - 100	24 - 31
	17	60	12.5	100	50 - 100	48 - 55
	20	70	14	130	50 - 160	60 - 76

Cycloid outer diameter and rated torque were set equal to the comparable harmonic drive diameter and maximum momentary peak torque. Remaining design parameters were chosen to achieve the maximum possible gear ratio that avoids undercutting and geometry constraints while staying within acceptable stress limits of the materials. These stress limits included a maximum roller double shear stress of 1.7 GPa, in accordance with ANSI B18.8.2, and 800 MPa Von Mises stress for remaining locations based on a safety factor of 2:1 for tempered SS440A. SKF (Göteborg, Sweden) needle roller bearing specifications were used to constrain the maximum allowable radial forces caused by the input cam. Cycloid disk thickness was chosen to match the resulting bearing thickness. Cycloid design tolerances were constructed using a conservative tolerance of +/- 0.025 mm per component, although harmonic drives report a tolerance of +/- 0.01 mm.

Calculated parameters included maximum gear ratio, efficiency, reflected input inertia, backlash, and gear ratio ripple. These calculations are described in [10]. Equation 7 was used to calculate efficiency, with a friction coefficient of 0.16 to represent the case of greased steel on steel.

B. Simulation Results

The cycloid drive design was able to achieve the same maximum gear ratio as harmonic drives in all but two cases (Table 2): the smallest and largest harmonic drive considered (CSF5 and CSD20). The CSF5 cycloid counterpart could only achieve a 70:1 gear ratio, and the CSD20 counterpart could only achieve a 130:1 gear ratio while avoiding intersection of rollers sufficiently large to withstand the high radial loads.

For all of the design comparisons considered, the maximum gear ratio of the cycloid drive was limited by the roller intersection constraint, which was a function of roller diameter. Roller diameter in turn was limited by shear stress where the roller interfaced with its collars.

The maximum stress always occurred at the shear plane of the roller, which is independent of the gear thickness or roller length. The thickness of the cycloid drive, as a result, was only limited by the thickness of the needle roller

bearings, resulting in a total transmission thickness of only 10-13mm. This cycloid thickness is comparable to the thickness of the CSD series, but substantially thinner than the CSF series, where thicknesses ranged from 16-37mm.

Cycloid drive estimated efficiency (84%) was greater than all of the harmonic drive maximum efficiencies (67–79%). It is important to note that cycloid drive efficiency remains constantly high, even at low torques, in contrast to the rated efficiency of harmonic drives, which drop off to 0% for small torques.

Cycloid drives consistently had lower reflected input inertia than their corresponding harmonic drives. The reflected cycloid inertia, often two orders of magnitude less than the harmonic drive, was achieved because the large component (cycloid disk) moved at output speed, contrasting with harmonic drives in which the wave generator moved at input speed.

Cycloid drives designs exhibited considerable backlash, ranging from 0.4° (CSD20) to 1.4° (CSF5), and substantially higher gear ratio ripple than the harmonic drives, ranging from 4% (CSD20) to 9% (CSF5). In contrast, none of the harmonic drives considered had backlash. Their minimal gear ratio ripple (unavailable for the CSF5) ranged from 0.7% (CSD20) to 0.9% (CSF8).

These design comparisons are tabulated in Table 2. Substantial advantages are emboldened.

Table 2
Harmonic vs. Cycloid Drives

Series		HD-CSF			HD-CSD		
		5	8	11	14	17	20
Max Gear Ratio	HD	**100**	100	100	100	100	**160**
	CD	70	100	100	100	100	130
Thickness	mm						
	HD	16	30	37	11	12.5	14
	CD	**10**	**10**	**11**	11	11	13
Max efficiency	%						
	HD	72	67	72	73	**79**	**79**
	CD	84	84	84	84	84	84
Input inertia	g cm^2						
	HD	0.25	3	12	21	54	90
	CD	**0.006**	**0.02**	**0.09**	**0.07**	**0.3**	**0.6**
Backlash	Deg	**HD**			*No backlash*		
	CD	1.4	0.9	0.9	0.6	0.4	0.4
GR$_f$	%	**HD**	**N.A.**	**0.9**	**0.7**	**0.7**	**0.7**	**0.7**
	CD	9	8	8	5	4	4

GR$_f$ is the periodic fluctuation in gear ratio

IV. EXPERIMENTAL ANALYSIS OF EFFICIENCY

A. Setup

Two 100:1 single-stage cycloid drives were made to assess the efficiency predictions of these models, as well as to measure the backdrivability of the cycloid drives. The two cycloid drives were identical (R = 30mm, R$_r$ = 0.8mm, e = 0.145 mm), except that in one the rollers were externally housed (Fig. 5 left), leading to predicted efficiency of 84% described by Eq. 7, and in the other the rollers were fused to the annulus (Fig. 5 right), leading to a decreased predicted efficiency of 64% described by Eq. 8. The cycloid disks and annuli were made from hardened (RC58-62) D2 tool steel using wire EDM manufacturing techniques. Roller diameters were increased from the actual size of 1.6mm to 1.65mm when creating the cycloid profile to take into account tolerance stack-up across the parts [10]. Wire EDM–cut gauge pins were used as rollers for the cycloid with externally housed (EH) rollers.

Both cycloid drives were fixed in a custom-built dynamometer (Fig. 6). A brushed motor (MicroMo 2657) with a 14:1 planetary gear train spun the cycloid input shaft at 143 RPM. A contactless torque sensor (Futek TRS 605) connected in series by flexible couplers between the motor shaft and cycloid shaft measured input torque. A magnetic particle brake (Placid Industries B222-24-1) applied current-dependent torque to the output shaft of the cycloid drive. Cycloid drives were run at 0.25 Nm of input torque (the continuous-torque limit of the motor) or 12Nm of output torque for one-hour to allow for break-in, followed by a slow ramp from zero to that same torque over the course of 20 minutes, during which time input and output torques were measured to calculate efficiency. Non-backdrivable torque was measured by hanging weights from a large pulley coupled to the cycloid output shaft.

B. Results

The efficiency of the cycloid with externally housed rollers was 71%, plus a 6 mNm input stiction term (Fig. 7). This efficiency was slightly less than the efficiency predicted by Eq. 7 and was relatively independent of applied torque. The efficiency of the cycloid with fused rollers was 42.3%, plus a 3 mNm stiction term. This efficiency was lower than predicted by Eq. 8, but its efficiency was also relatively independent of applied torque.

The cycloid drive with externally housed rollers had a non-backdrivable torque of 0.9 Nm. For a 100:1 gear ratio, this 9 mNm non-backdrivable torque matches well with the
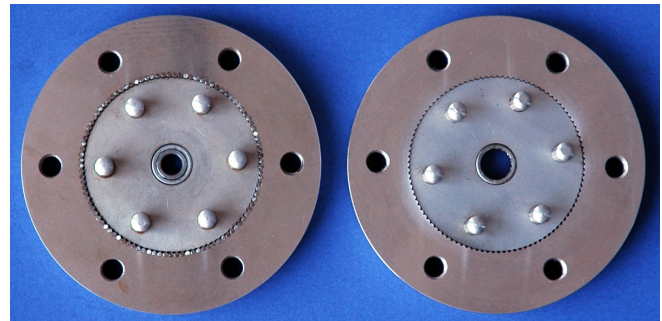

Fig. 5: Two 100:1 cycloid drives. Left: Externally housed rollers, similar to Fig. 4b. Right: Fused rollers, similar to Fig. 4c.
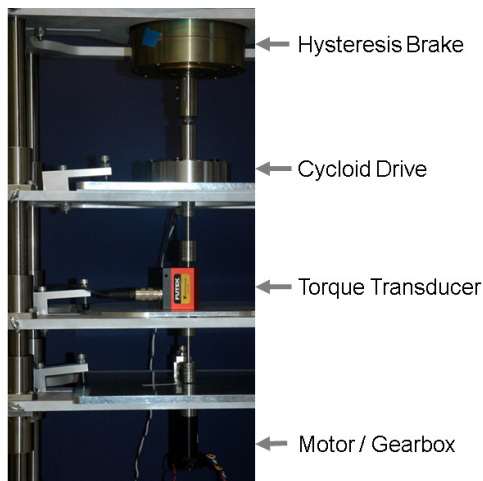
Fig. 6. Dynamometer

6 mNm stiction torque inherent in the cycloid.

V. DISCUSSION

Cycloid drives fitted into the same package diameter as harmonic drives with equal torque-generating capabilities. They demonstrated many advantages over harmonic drives, including substantially greater efficiency (especially at low torques) and lower reflected inertia, and often provided a thinner profile. These benefits were offset, however, by substantial disadvantages, including significant backlash and gear ratio ripple. In addition, in two out of six comparisons, cycloid drives were not able to obtain a gear ratio as high as the corresponding harmonic drive.

Both cycloid drives and harmonic drives are non-backdrivable for small torques (~1 Nm for cycloid drives and 5 Nm for harmonic drives), which is a function of their input stiction torque amplified by the gear ratio. Harmonic drives have greater stiction torque, and accordingly have larger non-backdrivable torques and poorer efficiencies at low torques—where stiction dominates—than cycloid drives. Although backdrivability has traditionally been beneficial in robotics, recent advances such as series elastic actuators [15] have allowed even non-backdrivable actuators to provide low impedances [16]. In applications such as
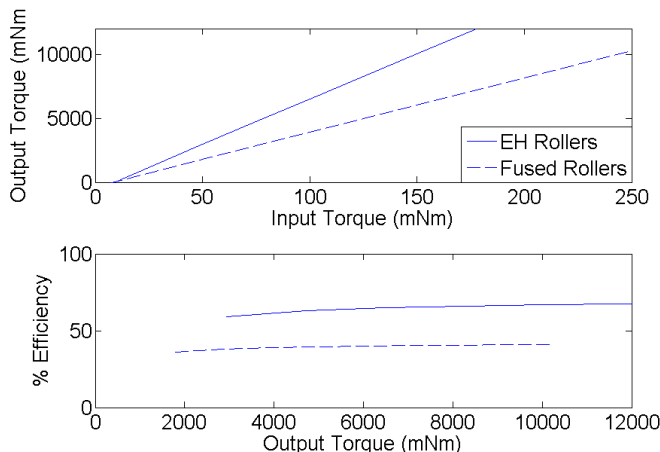

Fig. 7. Efficiency of two 100:1 cycloid drives suitable for compact robotic applications. Externally-housed (EH) had better efficiency than fused rollers.

prosthetics, non-backdrivability is a required feature so that joints can passively hold larger loads than their motors are capable of generating [17, 18].

Cycloid drives must be custom machined, unless a roller drive [19] or patented Ikona profile [20] is used. Roller drives present a viable alternative that replaces the custom cycloid lobe geometry with cylindrical rollers. Ikona gears, although allowing for standard machine tools, revert to sliding contact and substantially reduce the efficiency of the transmission. For custom applications in which commercially available harmonic drives are not suitable, harmonic drives are more difficult to machine than cycloid drives, due to their exotic three-dimensional S-shaped tooth profiles that are crucial to achieving the moderate efficiencies and high torques reported in this paper.

VI. CONCLUSION

Neither cycloid nor harmonic drives are universally superior for all applications and conditions. However, cycloid drives should be considered for applications in anthropomorphic robots and prostheses, especially those in which size, inertia, and efficiency take precedence over backlash and torque ripple.

REFERENCES

[1] J. M. Hollerbach*, et al.*, "A comparative analysis of actuator technologies for robotics," in *Robotics Review 2*, ed Cambridge, MA: MIT Press, 1991, pp. 299-342.
[2] J. K. Salisbury*, et al.*, "Preliminary design of a whole-arm manipulation system (wam)," presented at the 1988 IEEE International Conference on Robotics and Automation, Philadelphia, 1988.
[3] T. H. Massie and J. K. Salisbury, "The PHANTOM haptic interface: a device for probing virtual objects," presented at the Proceedings of the ASME Winter Annual Meeting, Symposium on Haptic Interfaces for Virtual Environment and Teleoperator Systems, Chicago, IL, 1994.
[4] A. Albu-Schaffer*, et al.*, "Soft robotics - From torque feedback-controlled lightweight robots to intrinsically compliant systems," *IEEE Robotics & Automation Magazine,* vol. 15, pp. 20-30, Sep 2008.
[5] T. Morita and S. Sugano, "Development of 4-D.O.F. Manipulator Using Mechanical Impedance Adjuster," presented at the International Conference on Robotics and Automation, Minneapolis, Minnesota, 1996.
[6] J. W. Sensinger and R. F. f. Weir, "Improved Torque Fidelity in Harmonic Drive Sensors through the Union of Two Existing Strategies," *IEEE/ASME Transactions on Mechatronics,* vol. 11, pp. 457-461, 2006.
[7] J. W. Sensinger and R. F. f. Weir, "User-Modulated Impedance Control of a Prosthetic Elbow in Unconstrained, Perturbed Motion," *IEEE Transactions on Biomedical Engineering,* vol. 55, pp. 1043-1055, 2008.
[8] H. D. Taghirad and P. R. Belanger, "Modeling and parameter identification of harmonic drive systems," *Journal of Dynamic Systems Measurement and Control-Transactions of the ASME,* vol. 120, pp. 439-444, DEC 1998.
[9] T. D. Tuttle, "Understanding and modeling the behavior of a harmonic drive gear transmission," M.S., Mechanical Engineering, Massachusetts Institute of Technology, 1992.
[10] J. W. Sensinger, "Unified approach to cycloid drive profile, stress, and efficiency optimization," *ASME Journal of Mechanical Design,* vol. 132, pp. 1-5, 2010.

[11]   J. H. Shin and S. M. Kwon, "On the lobe profile design in a cycloid reducer using instant velocity center," *Mechanism and Machine Theory,* vol. 41, pp. 596-616, May 2006.

[12]   D. C. H. Yang and J. G. Blanch, "Design and application guidelines for cycloid drives with machining tolerances," *Mechanism and Machine Theory,* vol. 25, pp. 487-501, 1990.

[13]   "Precision Planetary vs. Harmonic/Cycloidal drives," in *Get into gear*, B. P. Gearheads, Ed., ed. Port Washington, NY, 1997.

[14]   X. Li*, et al.*, "A new cycloid drive with high-load capacity and high efficiency," *Journal of Mechanical Design,* vol. 126, pp. 683-686, Jul 2004.

[15]   G. A. Pratt and M. M. Williamson, "Series elastic actuators," presented at the IEEE/RSJ International Conference on Intelligent Robots and Systems, Pittsburgh, PA, 1995.

[16]   J. W. Sensinger and R. E. F. Weir, "User-modulated impedance control of a prosthetic elbow in unconstrained, perturbed motion," *IEEE Transactions on Biomedical Engineering,* vol. 55, pp. 1043-1055, Mar 2008.

[17]   C. W. Heckathorne, "Components for electric-powered systems," in *Atlas of Amputations and Limb Deficiencies*, 3 ed Rosemont, IL: American Academy of Orthopaedic Surgeons, 2004, pp. 145-172.

[18]   R. F. f. Weir, "Design of Artificial Arms and Hands for Prosthetic Applications," in *Standard handbook of biomedical engineering and design*, M. Kutz, Ed., ed New York: McGraw-Hill, 2003, pp. 32.1-32.61.

[19]   T. S. Lai, "Geometric design of roller drives with cylindrical meshing elements," *Mechanism and Machine Theory,* vol. 40, pp. 55-67, 2005.

[20]   "IKONA," ed, 2009.